


Transcriptome Analysis Reveals the Putative Polyketide Synthase Gene Involved in Hispidin Biosynthesis in *Sanghuangporus sanghuang*

Jiansheng Wei^{a,b,t}, Liangyan Liu^{ct}, Xiaolong Yuan^b, Dong Wang^b, Xinyue Wang^{b,d}, Wei Bi^b, Yan Yang^e and Yi Wang^b 

^aHaba Snow Mountain Provincial Nature Reserve Management and Protection Bureau, Diqing, P.R. China; ^bLaboratory of Forest Plant Cultivation and Utilization, Yunnan Academy of Forestry & Grassland, Kunming, Yunnan, P.R. China; ^cCollege of Agronomy and Biotechnology, Yunnan Agriculture University, Kunming, Yunnan, P.R. China; ^dSchool of Pharmaceutical Science and Yunnan Key Laboratory of Pharmacology for Natural Products, Kunming Medical University, Kunming, P.R. China; ^eInstitute of Edible Fungi, Shanghai Academy of Agricultural Sciences, Shanghai, P.R. China

ABSTRACT

Hispidin is an important styrylpyrone produced by *Sanghuangporus sanghuang*. To analyze hispidin biosynthesis in *S. sanghuang*, the transcriptomes of hispidin-producing and non-producing *S. sanghuang* were determined by Illumina sequencing. Five PKSs were identified using genome annotation. Comparative analysis with the reference transcriptome showed that two PKSs (*ShPKS3* and *ShPKS4*) had low expression levels in four types of media. The gene expression pattern of only *ShPKS1* was consistent with the yield variation of hispidin. The combined analyses of gene expression with qPCR and hispidin detection by liquid chromatography-mass spectrometry coupled with ion-trap and time-of-flight technologies (LCMS-IT-TOF) showed that *ShPKS1* was involved in hispidin biosynthesis in *S. sanghuang*. *ShPKS1* is a partially reducing PKS gene with extra AMP and ACP domains before the KS domain. The domain architecture of *ShPKS1* was AMP-ACP-KS-AT-DH-KR-ACP-ACP. Phylogenetic analysis shows that *ShPKS1* and other PKS genes from Hymenochaetaceae form a unique monophyletic clade closely related to the clade containing Agaricales hispidin synthase. Taken together, our data indicate that *ShPKS1* is a novel PKS of *S. sanghuang* involved in hispidin biosynthesis.

ARTICLE HISTORY

Received 6 June 2023
Revised 20 August 2023
Accepted 30 August 2023

KEYWORDS

Sanghuangporus sanghuang;
transcriptome; hispidin
biosynthesis; polyketide
synthase; qRT-PCR

1. Introduction


Hispidin is a type of styrylpyrone, and it has antioxidant [1], antitumor [2,3], anti-inflammatory [4,5], antiviral [6], antiallergic [7], neuroprotective [8,9], antiangiogenic, and hypolipidemic properties [10,11]. Hispidin is a yellow pigment and was first isolated from *Inonotus hispidus* fungi [12]. Subsequently, hispidin has been identified in various fungal species of both the Hymenochaetaceae family, including species in the genera *Inonotus* (*I. obliquus*, *I. radiatus*, *I. xeranticus*), *Hymenochaete*, *Phellinus* [13], and *Sanghuangporus* [14], and the Hymenogastraceae family, including the genus *Gymnopilus* [15]. Hispidin and hispidin derivatives are also found in other fungal families such as the families Phaeolaceae [16], Omphalotaceae (*Neonothopanus nambi*) [17], Strophariaceae (*Hypholoma sublateritium*), and Cortinariaceae (*Cortinarius glaucopus*) [11]. Furthermore, hispidin derivatives were also identified

in some plants, including *Equisetum arvense* [18], *Pistacia atlantica* [19], *Leishmania amazonensis* [20], and *Goniothalamus umbrosus* [21].

A previous tracer study showed that styrylpyrone was derived from phenylalanine via cinnamic acid, *p*-coumaric acid, and caffeoyl coenzyme-A and that the pyrone ring is derived from acetate in fungi [22]. Polyketide synthase (PKS) is the key enzyme involved in styrylpyrone biosynthesis, which condenses one cinnamic acid or its derivatives with two malonyl-CoA molecules. PKSs usually are classified into three types according to their architecture [23]. Additionally, most fungal PKSs are type I PKSs with basic domains consisting of ketosynthase (KS), acyltransferase (AT), and acyl carrier protein (ACP) domains, and with additional catalytic domains, such as ketoreductase (KR), dehydratase (DH), enoylreductase (ER), methyltransferase (MeT), and thioesterase (TE). Fungal type I PKSs are also

CONTACT Yi Wang  wangyiyaf@126.com

[†]Jiansheng Wei and Liangyan Liu have contributed equally to this work.

 Supplemental data for this article can be accessed online at <https://doi.org/10.1080/12298093.2023.2257999>.

© 2023 The Author(s). Published by Informa UK Limited, trading as Taylor & Francis Group on behalf of the Korean Society of Mycology. This is an Open Access article distributed under the terms of the Creative Commons Attribution-NonCommercial License (<http://creativecommons.org/licenses/by-nc/4.0/>), which permits unrestricted non-commercial use, distribution, and reproduction in any medium, provided the original work is properly cited. The terms on which this article has been published allow the posting of the Accepted Manuscript in a repository by the author(s) or with their consent.

classified into aromatic or non-reducing PKSs, partially reducing PKSs, and highly reducing PKSs according to their domain architecture [24]. Several partially reducing PKSs were confirmed to be related to hispidin biosynthesis in bioluminescent and non-bioluminescent Agaricales [11]. In plants, a chalcone synthase (CHS) corresponding to a type III PKS has also been reported to be related to styrylpyrone biosynthesis in *Piper nigrum* [25]. Wu et al. [26] reported that a type III PKS (PmSPS1) from *Piper methysticum* catalyzed different substrates, such as hydrocinnamic acid, cinnamic acid, *p*-coumaric acid, and *p*-hydrocoumaric acid, into different styrylpyrones. However, it is still unclear that PKSs are involved in hispidin biosynthesis in Hymenochaetaceae family fungi.

Sanghuang is well-known medical fungus in China, Japan, and Korea. Sanghuang was once incorrectly called *Phellinus linteus*, but recently, after detailed morphological and molecular phylogenetic studies, Sanghuang has been given the correct binomial name *Sanghuangporus sanghuang* [27]. Sanghuang possesses antitumor [28], antioxidant [29], anti-inflammatory [30], hypoglycemic, hypolipidemic [31], and immunomodulatory activities [32]. The bioactive compounds of Sanghuang mainly are comprised of triterpenoids [33], polysaccharides [34], and flavonoids [35]. Hispidin is an important bioactive flavonoid of Sanghuang [14]. Although more than three genomes of Sanghuang have been assembled and the putative pathway of flavonoid biosynthesis has also been deduced, the specific PKS involved in hispidin biosynthesis in Sanghuang is still unclear.

In this study, the transcriptome data from *S. sanghuang* producing and non-producing hispidin were obtained by RNA-Seq. The putative PKS involved in hispidin production was identified by bioinformatics analysis, and then it was confirmed by combined analyses utilizing qRT-PCR and liquid chromatography mass spectrometry (LCMS) coupled with ion-trap and time-of-flight technologies (LCMS-IT-TOF).

2. Materials and methods

2.1. Fungal culture and growth conditions

The *S. sanghuang* strain SH1 was obtained from Yan Yang from the Institute of Edible Fungi, Shanghai Academy of Agricultural Sciences. Genotypic identification of the *S. sanghuang* SH1 strain was authenticated by the fungal ITS sequences according to a previous study [36].

Sanghuangporus sanghuang SH1 was inoculated into malt-yeast (MY) solid medium (Difco, Lawrence, KS, USA). Then, a mycelia agar block

(1 cm³) was transferred to 100 mL of new media. The carbon source of the media consisted of MY basal medium containing 2% (W/V) lactose (RT), mannitol (GLC), maltose (MYT), inositol (JC), glucose (PTT), and sorbitol (SLC), while the nitrogen sources of the media were prepared by the addition of 0.4% (W/V) of beef peptone (NRF), soy peptone (DDD), yeast extract (JMF), and malt extract (MYF) in the basal medium (maltose 1.8 g/L and glucose 6 g/L). The mycelia were harvested after cultivation at 28 °C for 2 weeks on a rotary shaker at 150 rpm.

2.2. LCMS analysis of hispidin

From the different culture media, *S. sanghuang* was collected by filtration and extracted using 100 mL of ethyl acetate. The extract was then evaporated with a Buchi Rotavapor (Buchi, Flawil, Switzerland). LCMS analyses were performed on the LCMS-IT-TOF system (Shimadzu, Kyoto, Japan) with an Agilent Eclipse Plus C18 column (100 × 2.1 mm i.d., 1.8 μm; Agilent Technologies, Santa Clara, CA, USA) at 30 °C. The injection volume was 2 μL for each LCMS analysis. MS experiments were conducted using an automatic pattern in positive ion mode. The Shimadzu Composition Formula Predictor was used to infer the molecular formula. For all *S. sanghuang* samples, hispidin production was confirmed through LCMS-IT-TOF analyses.

2.3. RNA extraction and sequencing library construction

The LCMS analysis showed that *S. sanghuang* produced hispidin when it was cultured in MY medium containing 2% (W/V) lactose (RT) and sorbitol (SLC), and *S. sanghuang* did not produce hispidin when it was cultured in basal medium containing 0.4% (W/V) soy peptone (DDD) and sorbitol (SLC). Therefore, the mycelial samples of *S. sanghuang* cultured in different mediums (RT, SLC, DDD, and JMF) were collected, and samples from three replicates of each treatment were subjected to Illumina sequencing. Firstly, the mycelial samples of three replicates of each treatment were collected together for RNA extraction. RNA was extracted with the Transzol Up Plus RNA Kit (Transgen Biotech, Beijing, China). The sequencing library was constructed using the NEBNext Ultra RNA Library Prep Kit for Illumina (NEB, Ipswich, MA, USA), and the library was analyzed by the Agilent 2100 Bioanalyzer (Agilent Technologies). The constructed library was sequenced using the Illumina platform (Illumina, San Diego, CA, USA). The sequencing depth of the independent samples was 6G. Raw reads (FASTQ format) were quality filtered using

FASTX-Toolkit61, and sequencing adaptors were removed with Trimmomatic. High-quality reads were mapped onto the reference genome of *S. sanghuang* (GCA_009806525.1) using HISAT2 [37].

2.4. Screening of differentially expressed genes

HTSeq statistics were used to compare the read count values of each gene with the original expression of the gene and to normalize gene expression using FPKM values (FPKM > 1). Analysis of differentially expressed genes (DEGs) was conducted using DESeq, with identification of DEGs according to the following criteria: $|\log_2(\text{expression fold change})| > 1$, $p < 0.05$.

2.5. Functional analysis of DEGs

All DEGs were mapped to each term of the GO database (<http://www.geneontology.org/>), and the number of genes associated with each GO term was determined. Using the list of the names and numbers for each GO term, the hypergeometric test was used to determine significantly enriched GO terms among DEGs compared to the genomic background. All differentially expressed genes were also mapped onto the KEGG pathway, with $Q\text{-value} \leq 0.05$ considered to be the threshold for significant enrichment by DEGs. Heatmaps were drawn using TBtools after normalizing the expression data.

2.6. Gene cloning and domain and phylogenetic analyses

Based on the transcriptome analysis, the genes with gene expression values of FPKM > 10 were *ShPKS1*, *ShPKS2*, and *ShPKS5*. Specific primers for gene cloning were designed based on the transcriptome sequences of these three *PKS* genes (Table S1). PCR was performed with super-fidelity DNA polymerase using cDNA as a template. The PCR product was cloned into the pUC19 vector with the pEASY-Uni Seamless Cloning and Assembly Kit (TransGen). Domain analysis was conducted using NCBI's conserved domain database. Three *PKS*s from *S. sanghuang* were aligned with 23 fungal *PKS* sequences retrieved from GenBank (Table S2). The alignment was analyzed using Muscle as implemented in the MEGA 7 program. To obtain a confidence value for the aligned sequence dataset, bootstrap analysis with 1000 replicates was performed using MEGA 7. A phylogenetic tree was constructed using the maximum likelihood method.

2.7. Real time quantitative fluorescence PCR

The expression of three *PKS* genes in the four different culture media was detected by q-PCR with special primers (Table S1). RNA from the different samples was extracted with the EasyPure[®] Plant RNA Kit (TransGen). Then, cDNA synthesis was performed with a reverse transcriptase kit (TaKaRa Super RT Kit; TaKaRa, Beijing, China). The gene expression was detected by fluorescence quantitative PCR with a PCR thermal cycler (ABI 7300; Applied Biological System, Foster City, CA, USA). The *tubulin* gene was used as an internal control gene. At least two independent biological replicates and three technical replicates for each biological replicate were analyzed by q-PCR for each sample to ensure reproducibility and reliability.

3. Results

3.1. Effects of different media on hispidin yield of *S. sanghuang*

The mycelia of *S. sanghuang* were inoculated into different media and cultivated with shaking for 2 weeks. Then, each culture medium was harvested and extracted with ethyl acetate. The crude extracts were detected by LCMS-IT-TOF. The detection of hispidin was confirmed by comparison to a reference sample (Sigma-Aldrich, St. Louis, MO, USA) with the same retention time ($t_R = 6.0$ min) and mass spectra (positive, m/z 247.0593, $[M + H]^+$, -2.5 mD; Figure S1) and UV spectrum (Figure S2). The detection results showed that the extracts of RT, SLC, and GLC cultures contained hispidin, while hispidin was not detected in MYT, JC, PTT, NRF, DDD, JMF, and MYF cultures (Figure 1).

3.2. RNA sequencing and read mapping onto *S. sanghuang* reference genome

Libraries constructed from *S. sanghuang* mycelia in media (RT, SLC, DDD, and JMF) were sequenced using the Illumina platform. From each of the four samples, we obtained at least 45,288,766 bp, and after filtering we obtained at least 41,019,250 bp. The total sequence similarity with the reference genome was higher than 94% and for Q20 and Q30 sequences, the similarity was >97 and >94%, respectively (Table 1). The raw data were deposited in NCBI with accession number SRX20095548.

In total, 12,307 protein-coding genes were predicted according to the reference genome. The predicted genes were annotated with known databases, and 6632 genes were annotated in the GO database, 3622 in the KEGG database, 8957 in the eggNOG database, and 7105 in the Swiss-Prot database. The

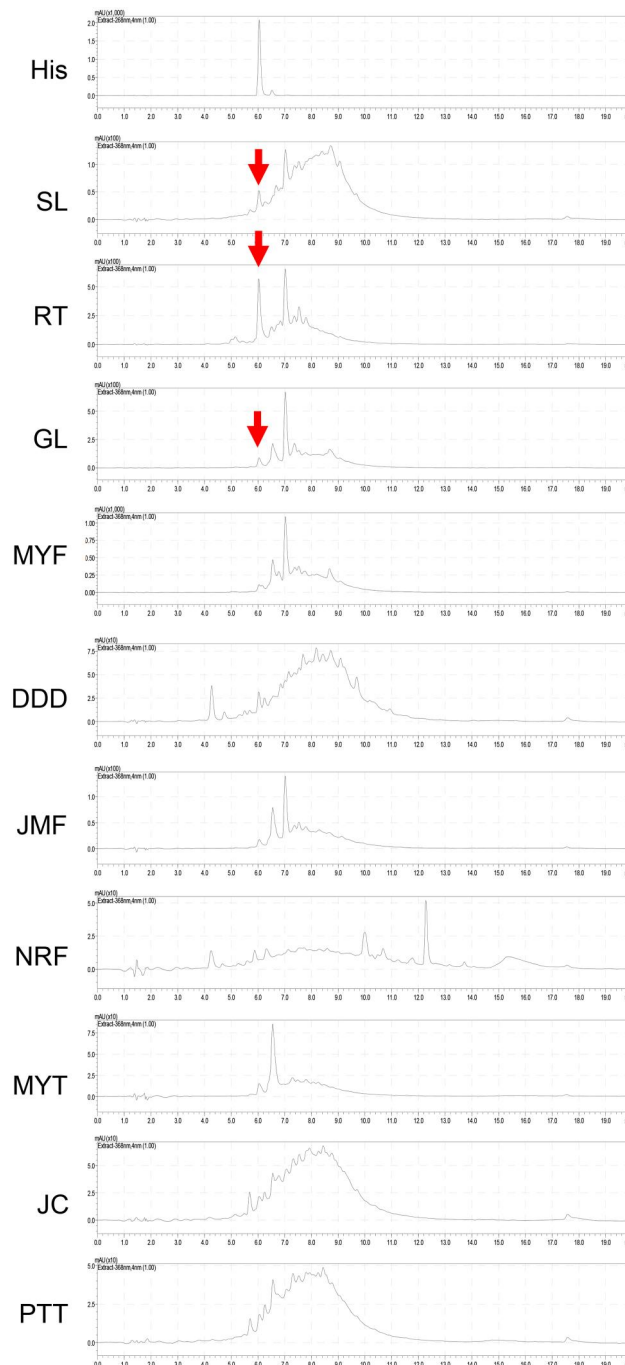


Figure 1. Detection of hispidin in extracts of different Sanghuang cultures. SLC, RT, GLC, MYF, DDD, JMF, NRF, MYT, JC, and PTT indicate different extracts from each different medium, respectively.

Table 1. Transcriptome sequencing data statistics.

Sample	Raw reads	Clean reads	Total mapped	Q20 (%)	Q30 (%)
SLC	45288766	41882100	39529649 (95.19%)	97.85	94.03
RT	48614202	43937560	40898845 (95.76%)	97.96	94.48
JMF	45501220	41019250	46162738 (94.90%)	97.83	94.38
DDD	53615258	49314890	37522071 (95.97%)	98.25	95.01

greatest number of genes was annotated in the NR database, with 12,016 (Figure 2).

3.3. Differentially expressed gene analysis

DEG analysis using DESeq identified a total of 2,077 DEGs (Figure 3), of which 308 were identified in the JMF_vs_DDD comparison (95 upregulated, 213

downregulated), 472 in the RT_vs_DDD comparison (226 upregulated, 246 downregulated), 342 in the RT_vs_JMF comparison (249 upregulated, 93 downregulated), 386 in the SLC_vs_DDD comparison (143 upregulated, 243 downregulated), 238 in the SLC_vs_JMF comparison (133 upregulated, 105 downregulated), and 331 in the SLC_vs_RT comparison (110 upregulated, 221 downregulated) (Figure 3, Table S3).

3.4. GO functional enrichment analysis of DEGs

To explore the functions of DEGs, we performed GO enrichment analysis on DEGs. The DEGs in the RT_vs_JMF comparison were classified into cellular

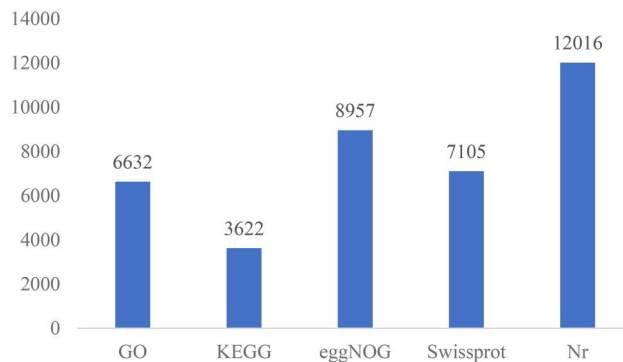


Figure 2. Gene function annotation.

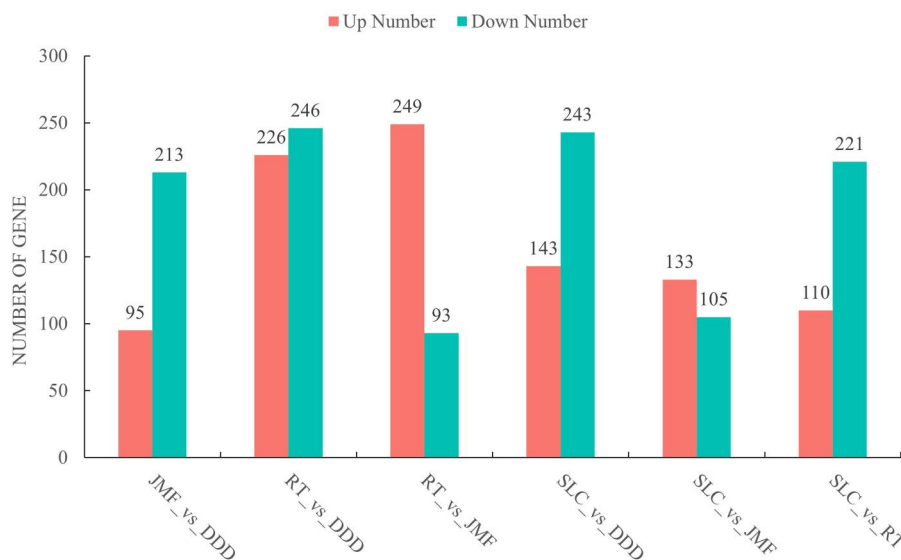


Figure 3. Statistical summary of the differentially expressed gene analysis.

component, molecular function, and biological process categories (Figure 4). The most significantly enriched category in both RT_vs_JMF and SLC_vs_JMF comparisons was oxidoreductase activity in the molecular function domain (Figure 4, Figure S4). The second most significant enrichment of the RT_vs_JMF and SLC_vs_JMF comparisons was iron ion binding and cofactor binding, respectively. The most significantly enriched term in the RT_vs_DDD and JMF_vs_DDD comparisons was transmembrane transport in the biological process domain (Figures S3 and S6). The most enriched term in the SLC_vs_DDD comparison was protein unfolding in the biological process domain (Figure S5). The most enriched term in the SLC_vs_RT category was the integral component of the membrane and intrinsic component of the membrane in the cellular component domain (Figure S7).

3.5. KEGG enrichment analysis of DEGs

To better understand the biological functions of DEGs, their enrichment in KEGG database pathways was analyzed. Among the DEGs in the RT_vs_JMF comparison, they were enriched in five categories including metabolism, genetic information

processing, cellular processes, environmental information processing, and human diseases. Most DEGs in the RT_vs_JMF comparison were enriched in metabolism, and their most significant enrichment was observed for pentose and glucuronate interconversions (Figure 5). Indeed, the main DEGs (from JMF_vs_DDD, RT_vs_DDD, SLC_vs_DDD, SLC_vs_JMF, and SLC_vs_RT comparisons) were annotated in the metabolism category (Figures S8–12). The most significant enrichment of the RT_vs_DDD comparison was pyruvate metabolism. The most and second most significant enrichments of the SLC_vs_DDD comparison were tyrosine metabolism and pyruvate metabolism, respectively. Additionally, the most significant enrichment of the SLC_vs_JMF comparison was ascorbate and aldarate metabolism. The most significant enrichment of the SLC_vs_RT comparison and JMF_vs_DDD was histidine metabolism and glycerolipid metabolism, respectively.

3.6. Transcriptome profiling of five PKS genes in different media

According to the genome annotation, there were five PKS genes in *S. sanghuang*. Transcriptome analysis showed that the genes *ShPKS3* and *ShPKS4* had a low

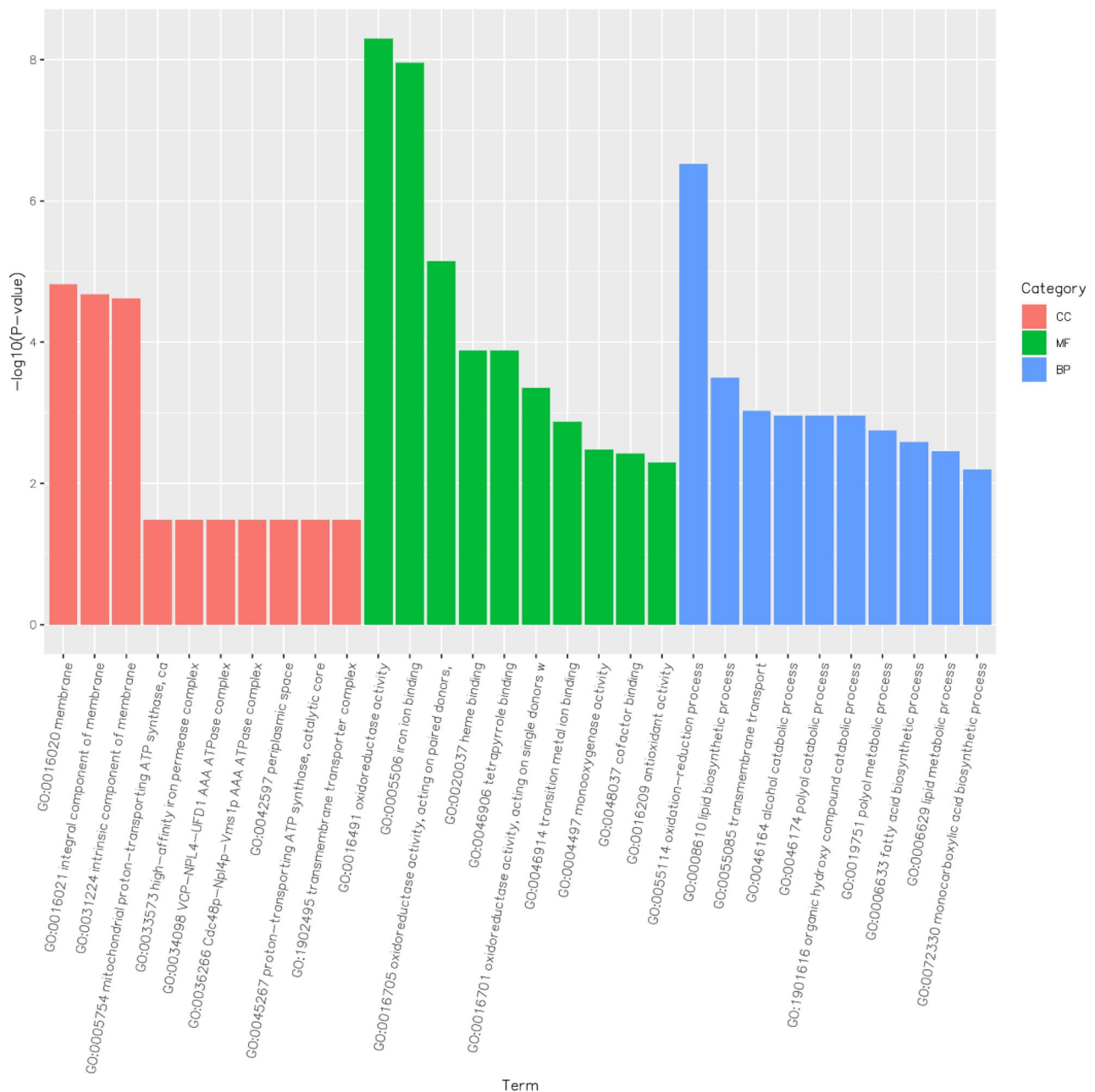


Figure 4. Gene ontology (GO) enrichment of the differentially expressed genes in the RT_vs_JMF comparison. The x-axis represents the GO terms, and the ordinate is $-\log_{10}(p\text{-value})$ of the enriched GO terms. CC, cellular component; MF, molecular function; BP, biological process.

expression level in all four medium cultures of *S. sanghuang*. The gene expression of *ShPKS5* was not significantly different among the four media. The expression of *ShPKS2* in DDD medium was higher than in the other three media (JMF, RT, and SLC). Additionally, the expression of *ShPKS1* cultured in both RT and SLC media was higher than in both DDD and JMF media. Only the expression pattern of *ShPKS1* was positively correlated with the yield of hispidin across the four media (Figure 6).

3.7. Gene cloning and domain architecture analysis

To confirm the transcriptome analysis results, the full cDNAs of *ShPKS1*, *ShPKS2*, and *ShPKS5* were

obtained by PCR with cDNA (Figure S13). The full cDNAs of *ShPKS3* and *ShPKS4* were not amplified by PCR (result not shown). Then, the obtained *PKS* was cloned into a vector. Three *PKS* genes were then confirmed by sequencing. The ORF of *ShPKS5* was a 6780 bp gene encoding a 2259 amino acid protein (accession number, OQ865374). Domain analysis showed that *ShPKS5* encodes a non-reducing *PKS*. Seven catalytic domains were identified in *ShPKS5* based on the presence of conserved motifs. It had starter unit acyltransferase (SAT), beta-ketoacyl-ACP synthase (KS), acyltransferase (AT), product template (PT), two acyl carrier protein (ACP), and thioesterase (TE) domains. The domain architecture of *ShPKS5* was SAT-KS-AT-PT-ACP-ACP-TE.

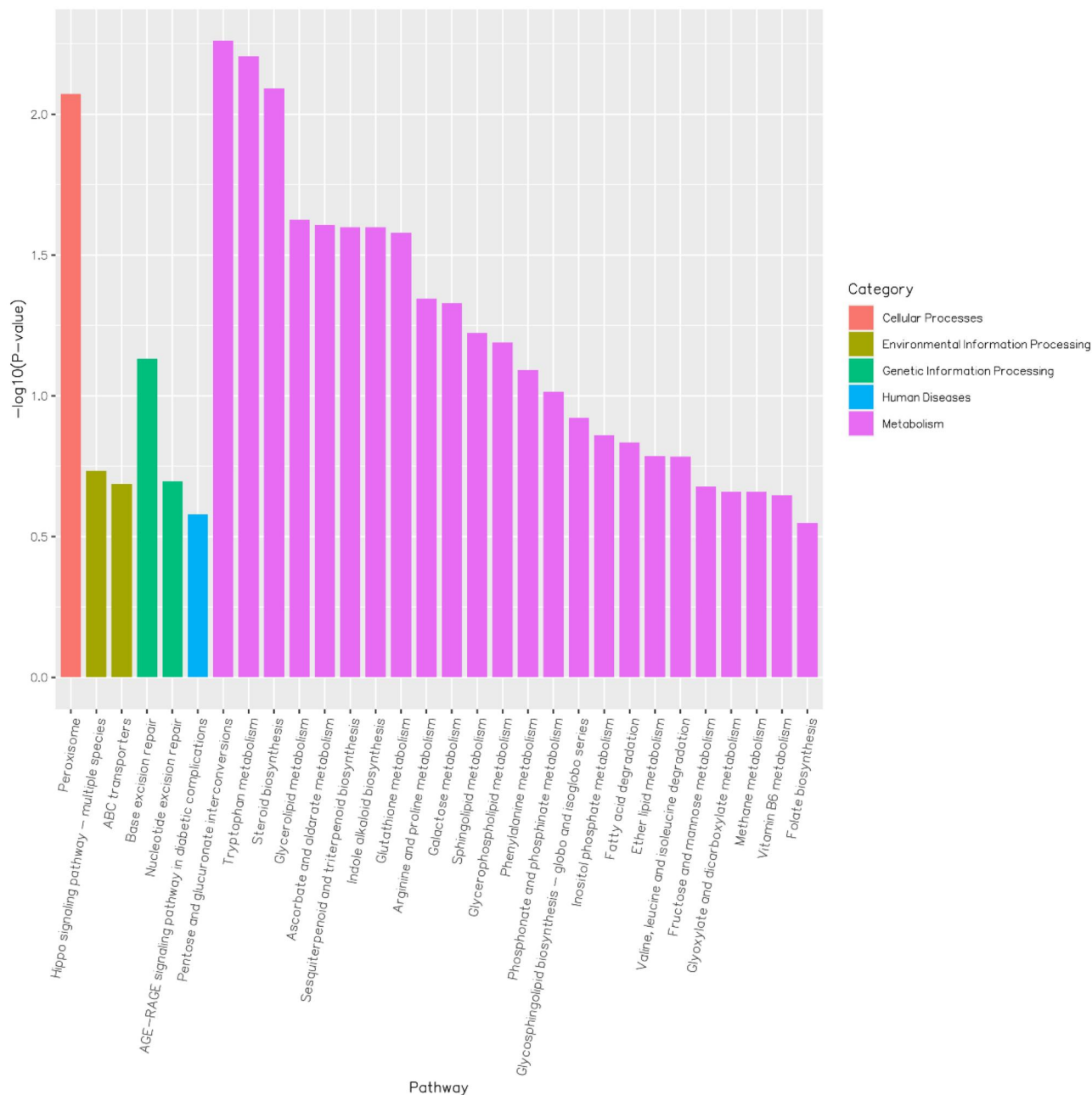


Figure 5. Kyoto encyclopedia of genes and genomes (KEGG) enrichment of differentially expressed genes in the RT_vs_JMF comparison. The x-axis represents the KEGG pathway, and the ordinate is the $-\log_{10}(p\text{-value})$ of the enriched KEGG terms.

The ORF of *ShPKS2* was a 5472 bp gene encoding an 1823 amino acid protein (accession number, OQ865373). Compared with *ShPKS5*, *ShPKS2* had one more dehydratase (DH) and β -ketoacyl reductase (KR) domain but no TE domain. The domain architecture of *ShPKS2* was KS-AT-DH-KR-ACP. Domain analysis showed that *ShPKS2* encodes a partially reducing PKS. A partially reducing PKS with this domain architecture (KS-AT-DH-KR-ACP) is usually involved in 6-methylsalicylic acid [38]. However, *ShPKS2* had more DH domains than common partially reducing PKSs, and it is thus a new type of partially reducing PKS.

The ORF of *ShPKS1* was a 7722 bp gene encoding a 2574 amino acid protein (accession number, OQ865372). *ShPKS1* also encodes a partially

reducing PKS. In contrast to *ShPKS5*, it had three ACP domains and an AMP domain. The domain architecture of *ShPKS1* was AMP-ACP-KS-AT-DH-KR-ACP-ACP. It is similar to the hispidin synthase of *H. sublateritium* (AMP-ACP-KS-AT-DH-KR-ACP) [11]. Thus, *ShPKS1* is a putative hispidin synthase in *S. sanghuang*.

3.8. Phylogenetic analysis of non-reducing PKSs

The amino acid sequence of the KS domain of three PKSs from *S. sanghuang* and several other fungal PKSs was used to generate multiple alignments and phylogenetic trees (Figure 3). The high-reducing PKSs of *Aspergillus niger* PKS1 and *A. tubingensis* PKS1 were the outgroup, and *ShPKS5* was grouped

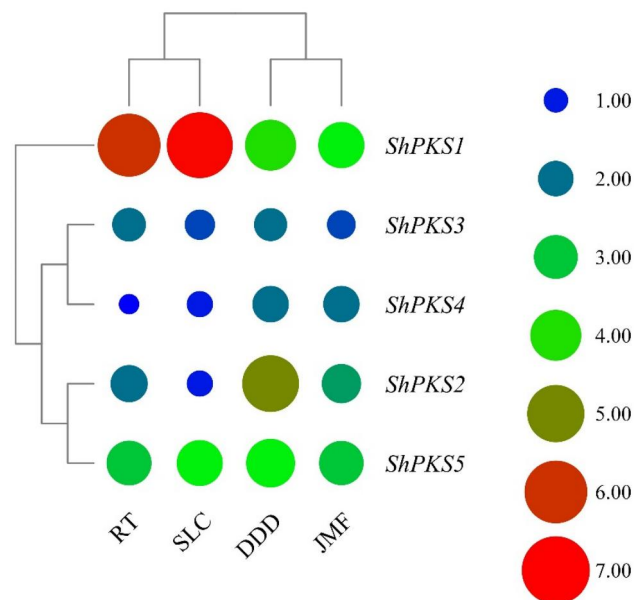


Figure 6. Heat map of five differentially expressed PKS genes of *Sanghuangporous sanghuang* in four media. The size and color indicate the level of gene expression. Large spot size and red color represent high expression, while small spot size and blue color represent low expression.

with *Sanghuangporous baumii* PKS2 and *I. obliquus* PKS2 into a unique clade. Additionally, the clade including ShPKS5 was the sister clade of orsellinic acid synthase. Thus, ShPKS1 and ShPKS1 belonged to a partially reducing PKS clade. The clade of ShPKS1, *S. baumii* PKS1, and *I. obliquus* PKS1 was the sister clade of hispidin synthase (Figure 7). The phylogenetic analysis also indicated that ShPKS1 is a putative hispidin synthase.

3.9. Expression patterns of PKS transcripts

To confirm the transcriptome analysis results, we assessed by q-PCR the expression of three PKS genes in different media (Figure 8). The q-PCR results showed that the expression of ShPKS5 in soy peptone (DDD) medium was slightly higher than in the other three mediums. Additionally, the expression of ShPKS5 in DDD medium was much higher than in the other three media. The gene expression of ShPKS1 in sorbitol (SLC) and lactose (RT) was much higher than in DDD and yeast extract (JMF). The qPCR results were thus consistent with transcriptome analysis.

4. Discussion

In fungi and plants, styrylpyrones and flavonoids are derived from phenylalanine. PKS plays an important role in the biosynthesis of styrylpyrones and flavonoids. In plants, the formation of the styrylpyrone scaffold is catalyzed by styrylpyrone synthase, a type III PKS (CHS-like) that condenses one hydroxycinnamoyl-CoA molecule with two malonyl-CoA molecules [25]. Chalcone formation, the most

crucial step in flavonoid biosynthesis, is catalyzed by a type III PKS (CHS) that condenses *p*-coumaroyl-CoA with three malonyl-CoA molecules [39]. Although type III PKS (CHS-like) has also been found in fungi, the known CHS-like PKS in fungi is not involved in styrylpyrone and flavonoid biosynthesis [39]. For example, the first fungal type III PKS to be functionally characterized was resorcylic acid synthase from *Neurospora crassa* [39]. In fungi, the functional similarity with CHS of plants is through a hybrid NRPS-PKS involved in flavonoid biosynthesis, which has a A-T-KS-AT-DH-KR-ACP-TE domain architecture [40–42]. Additionally, a hybrid PR-PKS is involved in styrylpyrone biosynthesis in fungi. Hispidin synthase was first characterized in bioluminescent Agaricales [43]. The hispidin synthase (Hisps) of bioluminescent fungi has a AMP-ACP-KS-AT-ACP domain architecture. Moreover, the Hisps in non-bioluminescent fungi has more DH and KR domains, and its domain architecture is AMP-ACP-KS-AT-DH-KR-ACP [11]. In the present study, we found that ShPKS1 (AMP-ACP-KS-AT-DH-KR-ACP-ACP) is a putative Hisps. It has one more ACP domain than known Hisps proteins. Thus, it may be a new kind of Hisps. The reported clustered genes are related to styrylpyrone and flavonoid biosynthesis in fungi [40,41,43]. However, we did not find this cluster of ShPKS1 genes in the genome analysis (result not shown). It is possible that there is a novel pathway of styrylpyrone biosynthesis utilized in *S. sanghuang*.

Although genome annotation results showed that five PKSs exist in the *S. sanghuang* genome, we only cloned three PKSs (ShPKS1, ShPKS2, and ShPKS5). It is possible that ShPKS3 and ShPKS4

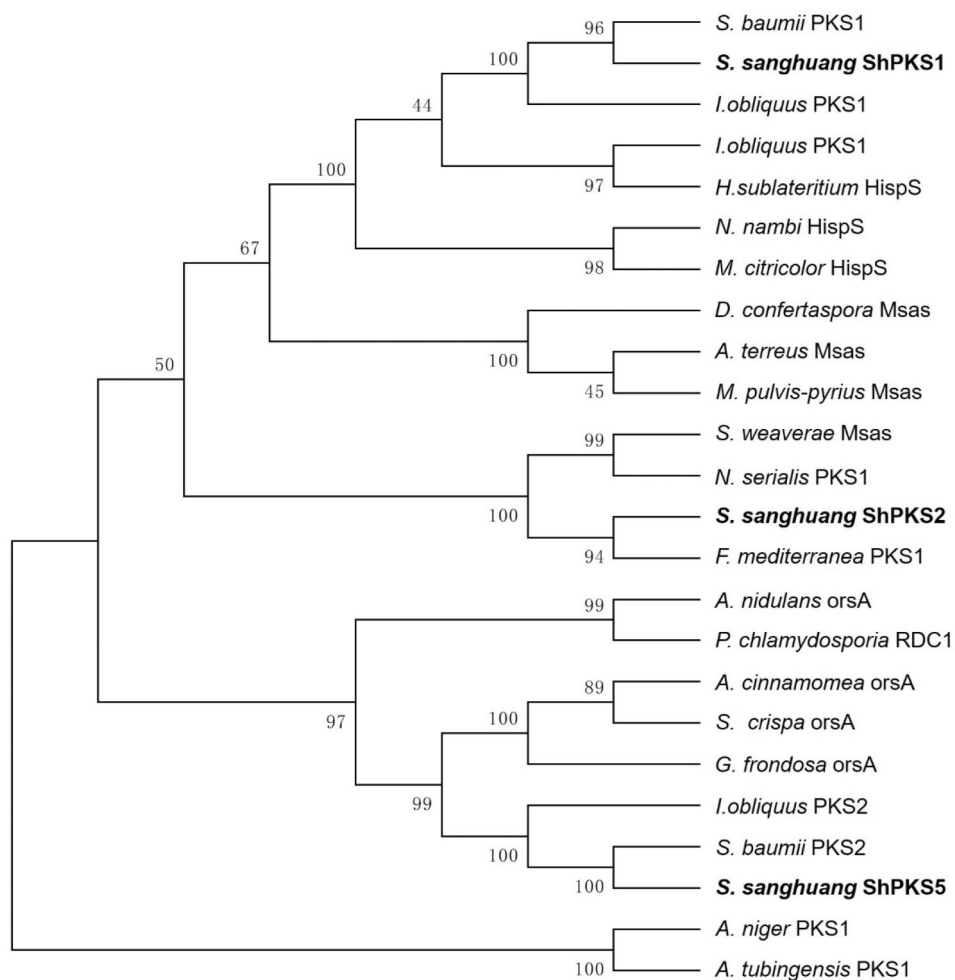


Figure 7. Phylogenetic relationship of *Sanghuangporous sanghuang* polyketide synthase (PKS) with other fungal PKSs. The deduced PKS protein was aligned with fungal PKS sequences retrieved from GenBank. The PKSs of the *S. sanghuang* clade obtained are marked in bold.

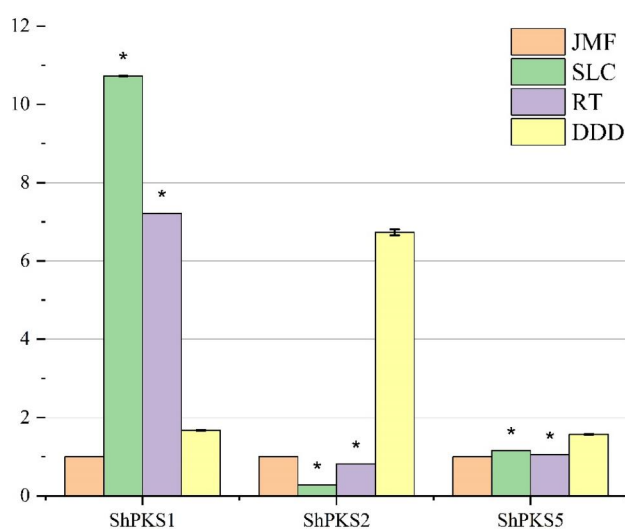


Figure 8. Gene expression of polyketide synthase (PKS) of *Sanghuangporous sanghuang* in different media.

had low expression levels in the cultured medium. The transcriptome analysis also showed low expression levels of *ShPKS3* and *ShPKS4*. Commonly, many genes and gene clusters are silenced under standard fermentation conditions [44]. The strategy of one-strain many compounds (OSMAC) has been

shown as a simple and powerful tool that can activate many silent biogenetic gene clusters in microorganisms to make more natural products [45]. In the future, we aim to utilize the OSMAC strategy to discover the function of silenced PKSs in *S. sanghuang*.

The culture conditions, such as media composition, temperature, osmolarity, and pH, influence the secondary metabolite production of fungi [46]. Li et al. [47] reported that different carbon sources influence the yield of hispidin in *P. linteus*, which produced a high yield of hispidin in glucose and yeast extract medium. However, we found *S. sanghuang* did not produce hispidin in a medium with glucose and yeast extract. This implies that there is a different regulatory mechanism in *S. sanghuang* and *P. linteus*.

Although several genomic studies deduced the pathway of hispidin biosynthesis in Hymenochaetaceae fungi, they did not deduce the specific PKS involved in hispidin biosynthesis [3,48–51]. In the present study, based on genome and transcriptome comparative analysis and combined analyses of gene expression and hispidin production, it was determined that ShPKS1 is involved in hispidin biosynthesis. This result identifies a specific PKS for subsequent confirmation of the function of hispidin synthase in *S. sanghuang* through gene silencing and heterologous expression.

5. Conclusions

We first confirmed *ShPKS1* was related to hispidin biosynthesis in *S. sanghuang*. Three different media were screened for the production of hispidin by *S. sanghuang* SH1. The function of *ShPKS1* was identified by combined analyses of gene expression with qPCR and hispidin detection by LCMS-IT-TOF. Domain analysis showed that *ShPKS1* is a partially reducing polyketide synthesis gene with extra AMP and ACP domains before its KS domain. The domain architecture of *ShPKS1* was determined to be AMP-ACP-KS-AT-DH-KR-ACP-ACP. Phylogenetic analysis also showed that *ShPKS1* and other PKS genes from Hymenochaetaceae form a unique clade that is closely related to the clade containing Agaricales hispidin synthase genes.

Disclosure statement

No potential conflict of interest was reported by the author(s).

Funding

The research was funded by General Project of Basic Research Program in Yunnan Province (project no. 202101AT070218), the National Natural Science Foundation of China (Project No. 31860177), and the Reserve Talents for Young and Middle-aged Academic and Technical Leaders of the Yunnan Province (Project No. 202205AC160044).

ORCID

Yi Wang  <http://orcid.org/0000-0003-3089-8184>

Data availability statement

Publicly available datasets were analyzed in this study. All newly generated sequences were deposited in GenBank with accession number SRX20095548.

References

- [1] El Hassane A, Shah ASA, Hassan NB, et al. Antioxidant activity of hispidin oligomers from medicinal fungi: a DFT study. *Molecules*. 2014; 19(3):3489–3507. doi: [10.3390/molecules19033489](https://doi.org/10.3390/molecules19033489).
- [2] Chandimali N, Jin WY, Huynh DL, et al. Combination effects of hispidin and gemcitabine via inhibition of stemness in pancreatic cancer stem cells. *Anticancer Res*. 2018;38(7):3967–3975. doi: [10.21873/anticancer.12683](https://doi.org/10.21873/anticancer.12683).
- [3] Zhang H, Chen R, Zhang J, et al. The integration of metabolome and proteome reveals bioactive polyphenols and hispidin in ARTP mutagenized *Phellinus baumii*. *Sci Rep*. 2019;9(1):16172. doi: [10.1038/s41598-019-52711-7](https://doi.org/10.1038/s41598-019-52711-7).
- [4] Shao HJ, Jeong JB, Kim KJ, et al. Anti-inflammatory activity of mushroom-derived hispidin through blocking of NF- κ B activation. *J Sci Food Agric*. 2015;95(12):2482–2486. doi: [10.1002/jsfa.6978](https://doi.org/10.1002/jsfa.6978).
- [5] Han YH, Chen DQ, Jin MH, et al. Anti-inflammatory effect of hispidin on LPS induced macrophage inflammation through MAPK and JAK1/STAT3 signaling pathways. *Appl Biol Chem*. 2020;63(1):1–9. doi: [10.1186/s13765-020-00504-2](https://doi.org/10.1186/s13765-020-00504-2).
- [6] Serseg T, Benarous K, Yousfi M. Hispidin and lepidine E: two natural compounds and folic acid as potential inhibitors of 2019-novel coronavirus main protease (2019-nCoV^{Mpro}), molecular docking and SAR study. *Curr Comput Aided Drug Des*. 2021;17(3):469–479. doi: [10.2174/1573409916666200422075440](https://doi.org/10.2174/1573409916666200422075440).
- [7] Tamrakar S, Fukami K, Parajuli GP, et al. Antiallergic activity of the wild mushrooms of Nepal and the pure compound hispidin. *J Med Food*. 2019;22(2):225–227. doi: [10.1089/jmf.2018.4267](https://doi.org/10.1089/jmf.2018.4267).
- [8] Chen W, Feng L, Huang Z, et al. Hispidin produced from *Phellinus linteus* protects against peroxynitrite-mediated DNA damage and hydroxyl radical generation. *Chem Biol Interact*. 2012; 199(3):137–142. doi: [10.1016/j.cbi.2012.07.001](https://doi.org/10.1016/j.cbi.2012.07.001).
- [9] Lai MC, Liu WY, Liou SS, et al. Hispidin in the medicinal fungus protects dopaminergic neurons from JNK activation-regulated mitochondrial-dependent apoptosis in an MPP⁺-induced in vitro model of parkinson's disease. *Nutrients*. 2023; 15(3):549. doi: [10.3390/nu15030549](https://doi.org/10.3390/nu15030549).
- [10] Lee S, Lee J, Choi K, et al. Polylactic acid and polycaprolactone blended cosmetic microneedle for transdermal hispidin delivery system. *Appl Sci*. 2021;11(6):2774. doi: [10.3390/app11062774](https://doi.org/10.3390/app11062774).
- [11] Palkina KA, Balakireva AV, Belozero OA, et al. Domain truncation in hispidin synthase orthologs from non-bioluminescent fungi does not lead to

- hispidin biosynthesis. *Int J Mol Sci.* 2023;24(2):1317. doi: [10.3390/ijms24021317](https://doi.org/10.3390/ijms24021317).
- [12] Edwards RL, Lewis DG, Wilson DV. 983. Constituents of the higher fungi. Part I. Hispidin, a new 4-hydroxy-6-styryl-2-pyrone from *Polyporus hispidus* (Bull.). *J. Chem. Soc.* 1961;4995–5002. doi: [10.1039/jr9610004995](https://doi.org/10.1039/jr9610004995).
- [13] Fiasson JL. Distribution of styrylpyrones in the basidiocarps of various hymenochaetaceae. *Biochem Syst Ecol.* 1982;10(4):289–296. doi: [10.1016/0305-1978\(82\)90002-3](https://doi.org/10.1016/0305-1978(82)90002-3).
- [14] Li IC, Chang FC, Kuo CC, et al. Pilot study: nutritional and preclinical safety investigation of fermented hispidin-enriched *Sanghuangporus sanghuang* mycelia: a promising functional food material to improve sleep. *Front Nutr.* 2021;8:788965. doi: [10.3389/fnut.2021.788965](https://doi.org/10.3389/fnut.2021.788965).
- [15] Lee IK, Cho SM, Seok SJ, et al. Chemical constituents of *Gymnopilus spectabilis* and their antioxidant activity. *Mycobiology.* 2008;36(1):55–59. doi: [10.4489/MYCO.2008.36.1.055](https://doi.org/10.4489/MYCO.2008.36.1.055).
- [16] Han JJ, Bao L, He LW, et al. Phaeolschidins A-E, five hispidin derivatives with antioxidant activity from the fruiting body of *Phaeolus schweinitzii* collected in the Tibetan Plateau. *J Nat Prod.* 2013;76(8):1448–1453. doi: [10.1021/np400234u](https://doi.org/10.1021/np400234u).
- [17] Oba Y, Suzuki Y, Martins GN, et al. Identification of hispidin as a bioluminescent active compound and its recycling biosynthesis in the luminous fungal fruiting body. *Photochem Photobiol Sci.* 2017;16(9):1435–1440. doi: [10.1039/c7pp00216e](https://doi.org/10.1039/c7pp00216e).
- [18] Beckert C, Horn C, Schnitzler JP, et al. Styrylpyrone biosynthesis in *Equisetum arvense*. *Phytochemistry.* 1997;44(2):275–283. doi: [10.1016/S0031-9422\(96\)00543-2](https://doi.org/10.1016/S0031-9422(96)00543-2).
- [19] Yousfi M, Djeridane A, Bombarda I, et al. Isolation and characterization of a new hispolone derivative from antioxidant extracts of *Pistacia atlantica*. *Phytother Res.* 2009;23(9):1237–1242. doi: [10.1002/ptr.2543](https://doi.org/10.1002/ptr.2543).
- [20] Fernandes NDS, Desoti VC, Dias A, et al. Styrylpyrone, isolated from an amazon plant, induces cell cycle arrest and autophagy in *Leishmania amazonensis*. *Nat Prod Res.* 2021;35(22):4729–4733. doi: [10.1080/14786419.2020.1715395](https://doi.org/10.1080/14786419.2020.1715395).
- [21] Abd Wahab NZ, Ibrahim N. Styrylpyrone derivative (SPD) extracted from *Goniothalamus umbrosus* binds to dengue virus serotype-2 envelope protein and inhibits early stage of virus replication. *Molecules.* 2022;27(14):4566. doi: [10.3390/molecules27144566](https://doi.org/10.3390/molecules27144566).
- [22] Perrin PW, Towers GHN. Hispidin biosynthesis in cultures of *Polyporus hispidus*. *Phytochemistry.* 1973;12(3):589–592. doi: [10.1016/S0031-9422\(00\)84448-9](https://doi.org/10.1016/S0031-9422(00)84448-9).
- [23] Shen B. Polyketide biosynthesis beyond the type I, II and III polyketide synthase paradigms. *Curr Opin Chem Biol.* 2003;7(2):285–295. doi: [10.1016/S1367-5931\(03\)00020-6](https://doi.org/10.1016/S1367-5931(03)00020-6).
- [24] Kroken S, Glass NL, Taylor JW, et al. Phylogenomic analysis of type I polyketide synthase genes in pathogenic and saprobic ascomycetes. *Proc Natl Acad Sci USA.* 2003;100(26):15670–15675. doi: [10.1073/pnas.2532165100](https://doi.org/10.1073/pnas.2532165100).
- [25] Heo KT, Lee B, Jang JH, et al. Construction of an artificial biosynthetic pathway for the styrylpyrone compound 11-methoxy-bisnoryangonin produced in engineered *Escherichia coli*. *Front Microbiol.* 2021;12:714335. doi: [10.3389/fmicb.2021.714335](https://doi.org/10.3389/fmicb.2021.714335).
- [26] Wu Y, Chen MN, Li S. De novo biosynthesis of diverse plant-derived styrylpyrones in *Saccharomyces cerevisiae*. *Metab Eng Commun.* 2022;14:e00195. doi: [10.1016/j.mec.2022.e00195](https://doi.org/10.1016/j.mec.2022.e00195).
- [27] Wu SH, Dai YC. Species clarification of the medicinal fungus sanghuang. *Mycosystema.* 2020;39(5):781–794.
- [28] Cheng J, Song J, Wang Y, et al. Conformation and anticancer activity of a novel mannogalactan from the fruiting bodies of *Sanghuangporus sanghuang* on HepG2 cells. *Food Res Int.* 2022;156(7):111336. doi: [10.1016/j.foodres.2022.111336](https://doi.org/10.1016/j.foodres.2022.111336).
- [29] Cai C, Ma J, Han C, et al. Extraction and antioxidant activity of total triterpenoids in the mycelium of a medicinal fungus, *Sanghuangporus sanghuang*. *Sci Rep.* 2019;9(1):1–10.
- [30] Lin WC, Deng JS, Huang SS, et al. Anti-inflammatory activity of *Sanghuangporus sanghuang* mycelium. *Int J Mol Sci.* 2017;18(2):347. doi: [10.3390/ijms18020347](https://doi.org/10.3390/ijms18020347).
- [31] Cheng J, Song J, Wei H, et al. Structural characterization and hypoglycemic activity of an intracellular polysaccharide from *Sanghuangporus sanghuang* mycelia. *Int J Biol Macromol.* 2020;164:3305–3314. doi: [10.1016/j.ijbiomac.2020.08.202](https://doi.org/10.1016/j.ijbiomac.2020.08.202).
- [32] Zhou LW, Ghobad-Nejhad M, Tian XM, et al. Current status of ‘sanghuang’ as a group of medicinal mushrooms and their perspective in industry development. *Food Rev Int.* 2022;38(4):589–607. doi: [10.1080/87559129.2020.1740245](https://doi.org/10.1080/87559129.2020.1740245).
- [33] Ma JX, Cai CS, Liu JJ, et al. In vitro antibacterial and antitumor activity of total triterpenoids from a medicinal mushroom *Sanghuangporus sanghuang* (agaricomycetes) in liquid fermentation culture. *Int J Med Mushrooms.* 2021;23(7):27–39. doi: [10.1615/IntJMedMushrooms.2021038916](https://doi.org/10.1615/IntJMedMushrooms.2021038916).
- [34] Li T, Chen L, Wu D, et al. The structural characteristics and biological activities of intracellular polysaccharide derived from mutagenic *Sanghuangporus sanghuang* strain. *Molecules.* 2020;25(16):3693. doi: [10.3390/molecules25163693](https://doi.org/10.3390/molecules25163693).
- [35] Li T, Mei Y, Li J, et al. Comparative compositions and activities of flavonoids from nine sanghuang strains based on solid-state fermentation and in vitro assays. *Fermentation.* 2023;9(3):308. doi: [10.3390/fermentation9030308](https://doi.org/10.3390/fermentation9030308).
- [36] Zhang XR, Zhang ZY, Wang Y, et al. Zn(II)2Cys6-type transcription factors in *Sanghuangporus sanghuang* grown under different carbon and nitrogen sources. *Mycosystema.* 2021;40(7):1676–1687.
- [37] Kim D, Langmead B, Salzberg SL. DHISAT: a fast spliced aligner with low memory requirements. *Nat Methods.* 2015;12(4):357–360. doi: [10.1038/nmeth.3317](https://doi.org/10.1038/nmeth.3317).
- [38] Fujii T, Yoshimoto H, Tamai Y. Acetate ester production by *Saccharomyces cerevisiae* lacking the ATF1 gene encoding the alcohol acetyltransferase. *J. Ferment. Bioeng.* 1996;81(6):538–542. doi: [10.1016/0922-338X\(96\)81476-0](https://doi.org/10.1016/0922-338X(96)81476-0).
- [39] Funo N, Awakawa T, Horinouchi S. Pentaketide resorcylic acid synthesis by type III polyketide synthase from *Neurospora crassa*. *J Biol Chem.* 2007;282(19):14476–14481. doi: [10.1074/jbc.M701239200](https://doi.org/10.1074/jbc.M701239200).

- [40] Zhang H, Li Z, Zhou S, et al. A fungal NRPS-PKS enzyme catalyses the formation of the flavonoid naringenin. *Nat Commun.* 2022;13(1):6361. doi: [10.1038/s41467-022-34150-7](https://doi.org/10.1038/s41467-022-34150-7).
- [41] Furumura S, Ozaki T, Sugawara A, et al. Identification and functional characterization of fungal chalcone synthase and chalcone isomerase. *J Nat Prod.* 2023;86(2):398–405. doi: [10.1021/acs.jnatprod.2c01027](https://doi.org/10.1021/acs.jnatprod.2c01027).
- [42] Zhang W, Zhang X, Feng D, et al. Discovery of a unique flavonoid biosynthesis mechanism in fungi by genome mining. *Angew Chem Int Ed Engl.* 2023;62(12):e202215529. doi: [10.1002/anie.202215529](https://doi.org/10.1002/anie.202215529).
- [43] Ke HM, Lee HH, Lin CYI, et al. *Mycena* genomes resolve the evolution of fungal bioluminescence. *Proc Natl Acad Sci USA.* 2020;117(49):31267–31277. doi: [10.1073/pnas.2010761117](https://doi.org/10.1073/pnas.2010761117).
- [44] Wasil Z, Pahirulzaman KAK, Butts C, et al. One pathway, many compounds: heterologous expression of a fungal biosynthetic pathway reveals its intrinsic potential for diversity. *Chem Sci.* 2013; 4(10):3845. doi: [10.1039/c3sc51785c](https://doi.org/10.1039/c3sc51785c).
- [45] Pan R, Bai XL, Chen JW, et al. Exploring structural diversity of microbe secondary metabolites using OSMAC strategy: a literature review. *Front Microbiol.* 2019;10:294. doi: [10.3389/fmicb.2019.00294](https://doi.org/10.3389/fmicb.2019.00294).
- [46] Hemphill CFP, Sureechatchaiyan P, Kassack MU, et al. OSMAC approach leads to new fusarielin metabolites from *Fusarium tricinctum*. *J Antibiot.* 2017;70(6):726–732. doi: [10.1038/ja.2017.21](https://doi.org/10.1038/ja.2017.21).
- [47] Li IC, Chen CC, Sheu SJ, et al. Optimized production and safety evaluation of hispidin-enriched *sanghuangporus sanghuang* mycelia. *Food Sci Nutr.* 2020;8(4):1864–1873. doi: [10.1002/fsn3.1469](https://doi.org/10.1002/fsn3.1469).
- [48] Huo J, Zhong S, Du X, et al. Whole-genome sequence of *Phellinus gilvus* (mulberry Sanghuang) reveals its unique medicinal values. *J Adv Res.* 2020;24:325–335. doi: [10.1016/j.jare.2020.04.011](https://doi.org/10.1016/j.jare.2020.04.011).
- [49] Shao Y, Guo H, Zhang J, et al. The genome of the medicinal macrofungus *sanghuang* provides insights into the synthesis of diverse secondary metabolites. *Front Microbiol.* 2019;10:3035. doi: [10.3389/fmicb.2019.03035](https://doi.org/10.3389/fmicb.2019.03035).
- [50] Jiang JH, Wu SH, Zhou LW. The first whole genome sequencing of *Sanghuangporus sanghuang* provides insights into its medicinal application and evolution. *JoF.* 2021;7(10):787. doi: [10.3390/jof7100787](https://doi.org/10.3390/jof7100787).
- [51] Duan Y, Han H, Qi J, et al. Genome sequencing of *Inonotus obliquus* reveals insights into candidate genes involved in secondary metabolite biosynthesis. *BMC Genomics.* 2022;23(1):314. doi: [10.1186/s12864-022-08511-x](https://doi.org/10.1186/s12864-022-08511-x).